IEEE Control Systems Letters paper presented at
2023 American Control Conference (ACC)
San Diego, CA, USA. May 31 - June 2, 2023

Distributed Cooperative Kalman Filter Constrained by Discretized Poisson Equation for Mobile Sensor Networks

Ziqiao Zhang, Scott T. Mayberry, Wencen Wu, and Fumin Zhang

Abstract— **This paper proposes cooperative Kalman filters for distributed mobile sensor networks where the mobile sensors are organized into cells that resemble a mesh grid to cover a spatial area. The mobile sensor networks are deployed to map an underlying spatial-temporal field modeled by the Poisson equation. After discretizing the Poisson equation with finite volume method, we found that the cooperative Kalman filters for the cells are subjected to a set of distributed constraints. The field value and gradient information at each cell center can be estimated by the constrained cooperative Kalman filter using measurements within each cell and information from neighboring cells. We also provide convergence analysis for the distributed constrained cooperative Kalman filter. Simulation results with a five cell network validates the proposed distributed filtering method.**

I. Introduction

Mobile sensor networks are effective for collecting information for natural processes such as hurricanes, ocean eddies and forest fires [1]–[4]. The natural processes are often modeled by physical parameters such as temperature, humidity, flow direction, flow speed, light intensity etc, which are functions of both space and time. They are called spatial-temporal fields, often satisfying various partial differential equations (PDE) derived from physics principles [5], [6].

The space and time are coupled in mobile sensing data because the data are collected along trajectories of the mobile sensors. Hence, mobile sensing data often need to be converted into a map, which are estimates of the spatial-temporal field. However, data collected by mobile sensors are subject to measurement noise. By combining the measurements from multiple sensors, the noise can be reduced so that a more accurate map of the underlying spatial-temporal field can be obtained [7]–[9].

Our previous work [10], [11] focused on solving the field mapping problem for mobile sensor networks. The movements of the mobile sensors are controlled so that they form a formation with approximately constant relative positions. We have derived the information dynamics, which model the change of the spatial-temporal field along the trajectory of the formation center. The information dynamics can be used to predict the field value along the trajectory of the formation center. The measurements of all the sensors are combined to provide an estimate of the field value at the formation center. A cooperative Kalman filter can be derived to fuse the prediction based on the information dynamics and the estimates obtained through combining all sensor measurements. In the case where the spatial-temporal field satisfies known PDEs, we discretize the PDEs into algebraic constraints on the field value at the formation center [11], [12]. Our recent work [13] proposes a constrained cooperative Kalman filter that is able to generate estimate of the field value that satisfies the constraints induced by the PDEs. This framework leads to a mapping solution using mobile sensor networks where the map is constructed along the trajectories of the formation center while at the same time satisfying the PDEs.

In this paper, we generalize the cooperative Kalman filter with PDE induced constraints to distributed mobile sensor networks where a larger number of sensors are involved. The major advancement from our previous work is that we organize mobile sensors to form multiple cells. For each cell, only sensor measurements pertaining to that cell are used to estimate the field value at the center of the cell. The estimated information at cell center will be shared among neighboring cells. The collection of cells will form a mesh that covers a larger area than a single formation. This new formulation is welcome in practice because the sensor power can be better distributed spatially. As a result, the map constructed will be along the trajectories of a collection of cell centers rather than a single formation center.

Under the distributed setting, field values at the cell centers are related by the PDEs. Hence a major challenge is to properly discretize the PDEs so that the constraints on the field values at the cell centers can be well formulated. We are motivated by the finite volume methods (FVM) introduced by [14] that has found broad applications in numerical computation of PDEs [15]. A mesh grid is first constructed to cover the configuration space, then the FVM offers a systematic way of discretizing the PDE over the mesh grid. For a mobile sensor network, each node can be viewed as a grid point in the mesh grid, providing measurements of the field value at the grid point. Leveraging the FVM, we demonstrate a discretization of the Poisson equation that can be used as constraints for the cooperative Kalman filter.

Our major contribution is the development of the cooperative Kalman filter constrained by the Poisson equation for a mobile sensor network with large number of sensors. Given the popularity of the FVM, this method can be generalized to handle constraints imposed by other types of PDEs [16].

The research work is supported by ONR grants N00014-19-1-2556 and N00014-19-1-2266; AFOSR grant FA9550-19-1-0283; NSF grants GCR-1934836, CNS-2016582, ITE-2137798, CMMI-1917300, and RINGS-2148353; and NOAA grant NA16NOS0120028.

Ziqiao Zhang, Scott T. Mayberry and Fumin Zhang are with the School of Electrical and Computer Engineering, Georgia Institute of Technology, Atlanta, GA 30308, USA. Wencen Wu is with the Computer Engineering Department of San Jose State University, San Jose, CA 95192, USA. Email: ziqiao.zhang@gatech.edu, mayberry@gatech.edu, wencen.wu@sjsu.edu, fumin@gatech.edu

We show that the cooperative Kalman filter can also be computed in a distributed fashion with provable convergence. These contributions provide a general framework for state estimation using a large distributed mobile sensor network.

II. Problem Formulation

In this section, we will formulate the estimation problem of field value and gradient along trajectory using distributed mobile sensor networks for a spatial-temporal field in d-dimensional space, where $d \in \mathbb{Z}_+$ and $d \geq 2$.

We assume that the field can be described by the following Poisson equation in a spatial domain $\Omega \subseteq \mathbb{R}^d$

$$\nabla^2 z(r,t) = f(r), \tag{1}$$

where $r \in \Omega$ represents location, $t \in \mathbb{R}_+$ represents time, $z(\cdot,\cdot) : \mathbb{R}^d \times \mathbb{R}_+ \to \mathbb{R}$ is the field function, and ∇^2 is the Laplacian operator. Function $f(\cdot) : \mathbb{R}^d \to \mathbb{R}$ is spatial varying, not depending on time t and assumed to be known. The equation (1) has the initial condition $z(r,0) = z_0(r)$ for $r \in \Omega$, and the boundary condition $z(r,t) = z_b(r,t)$ for $r \in \partial\Omega$, where $z_0(r)$ and $z_b(r,t)$ are arbitrary initial condition and Dirichlet boundary condition, respectively.

Suppose a group of mobile sensors are employed in the field described by (1), taking discrete measurements of the field $z(r,t)$ in a distributed way. These mobile sensors have limited communication so that they can only share information with their neighbors instead of everyone in the network. Based on the information sharing, the mobile sensors form communication cells with neighbors and serve as vertices of these cells, as illustrated by Fig. 1

Assumption II.1 *The mobile sensors keep fixed communication graph and fixed formation shape while moving in the field. The spatial domain covered by the mobile sensor network is defined as Ω_r with boundary $\partial\Omega_r$.*

Remark II.2 *In this way, the communication cells have fixed shapes and fixed mobile sensors as vertices. Each mobile sensor belongs to fixed communication cell(s), where the number of cells sharing the same mobile sensor can be greater than 1, as shown in Fig. 1.*

Assumption II.3 *There is no overlap between any communication cells. The intersection between two cells can only be edges connecting two vertices of the communication graph.*

Definition II.4 *Two communication cells are called neighboring cells if they have shared edge(s) on the cell boundaries, e.g. C_1, C_2 in Fig. 1.*

Assumption II.5 *Every communication cell has at least one neighboring cell. Within each communication cell, the information sharing is all-to-all among agents. The information sharing among different communication cells only happens between neighboring cells and the shared information is the estimated information at cell centers.*

Suppose the mobile sensors form multiple communication cells denoted as $C_1, C_2, \cdots, C_N$. Denote the ith mobile sensor on cell C_j as (i,j) and the location of this mobile sensor

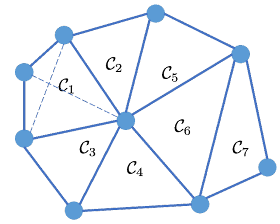

Fig. 1. Example of 7 communication cells with 9 agents, where the blue nodes represent the agents and lines connecting two nodes represent communication between two mobile sensors. Solid lines represent boundary edges of a cell and dashed ones represent communication inside one cell.

at time step t_k as $r^k_{i,j}$. Then the noisy measurement $p(r^k_{i,j},k)$ taken by this agent at $(r^k_{i,j},t_k)$ can be written as

$$p(r^k_{i,j},k) = z(r^k_{i,j},k) + n^k_{i,j}, \tag{2}$$

where $n^k_{i,j} \in \mathbb{R}$ is an i.i.d. Gaussian noise with zero mean. Define the center location of cell C_j at t_k as $r^k_{c_j}$ and $r^k_{c_j} = \frac{1}{|C_j|}\sum_{i\in C_j} r^k_{i,j}$, where $|C_j|$ is the number of mobile sensors belonging to cell C_j. One of our goals in this work is to estimate field value $z(r_{c_j},t)$ and corresponding gradient $\nabla z(r_{c_j},t)$ along trajectory.

Since the measurements taken by the mobile sensors are discrete, the continuous PDE model (1) should be discretized properly. The area covered by the sensor network can be partitioned by the communication cells which resembles a mesh grid for the FVM [14]. Thus, another goal of this work is to discretize the PDE model using FVM to establish algebraic relationships among the field values at cell centers.

In order to solve the distributed state estimation problem, we will work on two subproblems: 1) Discretize the PDE model using FVM for each communication cell. 2) Estimate field value and corresponding gradient at each cell center along trajectory.

Our proposed solution follows a distributed constrained cooperative Kalman filter strategy, where field value along with corresponding gradient at each cell center are treated as information states and the discretized PDE will be incorporated as state constraint. The constraint will build the connections between each individuals cells.

III. Information Dynamics and Measurement Equations

In this section, we will review the information dynamics at cell center $r^k_{c_j}$ of C_j and the measurement equations for mobile sensors from C_j at time step t_k, respectively.

A. Information Dynamics

At the cell center $r^k_{c_j}$ for any cell C_j, we have the following approximations [10] $z(r^{k+1}_{c_j},k+1) \approx z(r^k_{c_j},k) + (r^{k+1}_{c_j} - r^k_{c_j})^\intercal \nabla z(r^k_{c_j},k)$, $\nabla z(r^{k+1}_{c_j},k+1) \approx \nabla z(r^k_{c_j},k) + \nabla^2 z(r^k_{c_j},k)(r^{k+1}_{c_j} - r^k_{c_j}) = \nabla z(r^k_{c_j},k) + f(r^k_{c_j})(r^{k+1}_{c_j} - r^k_{c_j})$, where the last equality is given by PDE model in (1).

Define state variable $x(j,k) = [z(r^k_{c_j},k), \nabla z(r^k_{c_j},k)]^\intercal$, and we can get the following state equation

$$x(j,k+1) = A(j,k)x(j,k) + U(j,k) + e(j,k), \tag{3}$$

where $A(j,k) \triangleq \begin{bmatrix} 1 & (r_{c_j}^{k+1}-r_{c_j}^{k})^{\intercal} \\ 0_{d\times 1} & I_{d\times d} \end{bmatrix}$, $U(j,k) \triangleq \begin{bmatrix} 0 \\ f(r_{c_j}^{k})(r_{c_j}^{k+1}-r_{c_j}^{k}) \end{bmatrix}$ and $e(j,k)$ is the noise term.

B. Measurement Equation

For a given cell C_j, we consider a mobile sensor i belonging to this cell. Then the field value at $r_{i,j}^k$ can be locally approximated using a Taylor series as

$$\begin{aligned} z(r_{i,j}^k,k) \approx\, & z(r_{c_j}^k,k) + (r_{i,j}^k - r_{c_j}^k)^{\intercal}\nabla z(r_{c_j}^k,k) \\ & + \frac{1}{2}(r_{i,j}^k - r_{c_j}^k)^{\intercal} H(r_{c_j}^k,k)(r_{i,j}^k - r_{c_j}^k). \end{aligned} \tag{4}$$

Let $Z(j,k) = [z(r_{1,j}^k,k),\cdots,z(r_{|C_j|,j}^k,k)]^{\intercal}$ be the vector of true field values at the mobile sensor locations of the cell C_j. Define

$$C(j,k) \triangleq \begin{bmatrix} 1 & (r_{1,j}^k - r_{c_j}^k)^{\intercal} \\ \vdots & \vdots \\ 1 & (r_{|C_j|,j}^k - r_{c_j}^k)^{\intercal} \end{bmatrix}, D(j,k) \triangleq \begin{bmatrix} \frac{1}{2}(((r_{1,j}^k - r_{c_j}^k)\otimes(r_{1,j}^k - r_{c_j}^k))^{\intercal} \\ \vdots \\ \frac{1}{2}((r_{|C_j|,j}^k - r_{c_j}^k)\otimes(r_{|C_j|,j}^k - r_{c_j}^k))^{\intercal} \end{bmatrix},$$

where $\otimes$ is the Kronecker product. The Taylor approximations (4) for all sensors from cell C_j can be written as

$$Z(j,k) = C(j,k)x(j,k) + D(j,k)H(j,k), \tag{5}$$

where $H(j,k)$ is a column vector obtained by rearranging elements of the Hessian $H(r_{c_j}^k,k)$.

Let $\hat{H}(j,k)$ represent the estimate of the Hessian vector $H(j,k)$ at cell center $r_{c_j}^k$, equation (2) can be rewritten as

$$\begin{aligned} P(j,k) = &\, C(j,k)x(j,k) + D(j,k)\hat{H}(j,k) \\ & + D(j,k)\varepsilon(j,k) + \boldsymbol{n}(j,k), \end{aligned} \tag{6}$$

where $P(j,k) = [p(r_{1,j}^k,k),\cdots,p(r_{|C_j|,j}^k,k)]^{\intercal}$ is the measurement vector, $\varepsilon(j,k)$ is the Hessian estimation error, and $\boldsymbol{n}(j,k)$ is the vector of noise $n_{i,j}^k$ in (2). Hessian estimation will follow the procedure of cooperative estimation in [10], and we will not discuss the estimation details in this paper.

IV. Approximation Based on FVM

In this section, we will apply the FVM from [14] to obtain approximation for each individual cell C_j. Each cell is composed by vertices of mobile sensors and edges connecting two sensors. The edges can be characterized into two types: edges not on the boundary of the mobile sensor networks, and boundary edges of the mobile sensor networks. Then the cells can also be divided into two types: cells containing no boundary edges (cell C_6 in Fig. 1), and cells containing boundary edges (cells $C_1,\cdots,C_5$ in Fig. 1). All the values in this section are at the same time step t_k, so we will drop time index k for simplicity.

A. Cells Containing no Boundary Edges of the Network

Suppose cell C_j contains no boundary edges of the network, and every boundary edge of C_j is shared by C_j and one of its neighboring cell. Consider a shared edge s by C_j and neighboring cell $C_{j'}$. Denote the cell centers for $C_j, C_{j'}$ as $c_j, c_{j'}$, respectively. Denote the two vertices of edge s as $a_i, a_{i'}$. As shown in Fig. 2, denote $\nu_{jj'}$ as the unit outward normal vector on edge s connecting a_i and $a_{i'}$ with $\tau_{jj'}$ as the corresponding unit counterclockwise tangent vector, and denote $\nu_{ii'}$ as the unit outward normal vector on edge connecting c_j and $c_{j'}$ with $\tau_{ii'}$ as the corresponding unit counterclockwise tangent vector. Define θ_s to be the angle between $\nu_{jj'}$ and $\tau_{ii'}$.

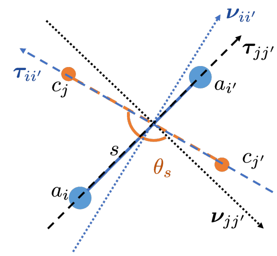

Fig. 2. Illustration of $\nu_{jj'}, \tau_{jj'}, \nu_{ii'}, \tau_{ii'}, \theta_s$ with given cell centers $c_j, c_{j'}$ and given edge s connecting vertices $a_i, a_{i'}$. Orange nodes represent cell centers.

Then we can obtain the following relationship

$$\nu_{jj'} = -\tan\theta_s \tau_{jj'} + \frac{1}{\cos\theta_s}\tau_{ii'}, \tag{7}$$

By taking integrals of (1) over cell C_j, we can obtain

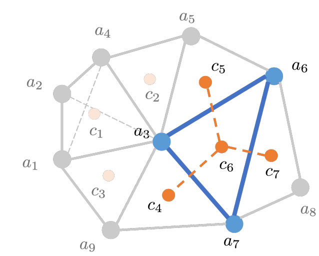

Fig. 3. Example of cell containing no network boundary edges, which is C_6 in Fig. 1. Denote cell centers as $c_1,\cdots,c_7$ and vertices as $a_1,\cdots,a_9$. Then $\int\int_{C_6}\nabla^2 z$ will use z values at $a_3, a_6, a_7, c_4, c_5, c_6, c_7$ according to equation (8). Orange nodes represent cell centers and orange dashed lines represent information sharing of cell centers from neighboring cells.

$\int\int_{C_j}\nabla^2 z = \sum_{s\in\partial C_j}\int_{S_{jj'}}\nabla z\cdot\nu_{jj'} = \int\int_{C_j} f$. Substituting $\nu_{jj'}$ by (7) leads to $\sum_{s\in\partial C_j} -\tan\theta_s\int_{S_{jj'}}\nabla z\cdot\tau_{jj'} + \frac{1}{\cos\theta_s}\int_{S_{jj'}}\nabla z\cdot\tau_{ii'} = \int\int_{C_j} f$. By finite difference method, we know that $\int_{S_{jj'}}\nabla z\cdot\tau_{jj'} \approx z_{a_i} - z_{a_{i'}}$, $\int_{S_{jj'}}\nabla z\cdot\tau_{ii'} \approx \frac{|S_{jj'}|}{|S_{ii'}|}(z_{c_{j'}} - z_{c_j})$. This will lead to

$$\sum_{s\in\partial C_j}[-\tan\theta_s(z_{a_i} - z_{a_{i'}}) + \frac{|S_{jj'}|}{\cos\theta_s|S_{ii'}|}(z_{c_{j'}} - z_{c_j})] = \int\int_{C_j} f. \tag{8}$$

B. Cells Containing Boundary Edge(s) of the Network

Suppose cell C_m contains network boundary edge(s). For the shared edges between C_m and neighboring cells, we apply the same approach as that described in Fig. 2. In this part, we consider a boundary edge s' with vertices $a_n, a_{n'}$. Denote the middle point of edge s' as c'_m. Define unit outward normal vectors $\nu_{mm'}, \nu_{nn'}$ and corresponding unit counterclockwise tangent vectors $\tau_{mm'}, \tau_{nn'}$ as shown in Fig. 4. Then we can obtain $\nu_{mm'} = -\tan\theta_s\tau_{mm'} + \frac{1}{\cos\theta_{s'}}\tau_{nn'}$. By taking integrals of (1) over cell C_m, we have $\int\int_{C_m}\nabla^2 z = \sum_{s\in\partial C_m}\int_{S_{mm'}}\nabla z\cdot\nu_{mm'} = \int\int_{C_m} f$. This leads to $\sum_{s\in\partial C_m} -\tan\theta_{s'}\int_{S_{mm'}}\nabla z\cdot\tau_{mm'} + \frac{1}{\cos\theta_{s'}}\int_{S_{mm'}}\nabla z\cdot\tau_{nn'} = \int\int_{C_m} f$.

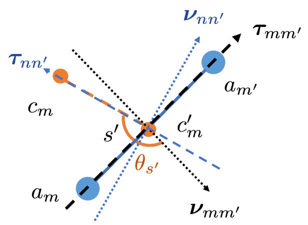

Fig. 4. Illustration of cell containing network boundary edge(s).

By finite difference method, we can obtain that $\int_{S_{mm'}} \nabla z \cdot \tau_{mm'} \approx z_{a_n} - z_{a_{n'}}$ and

$$\int_{S_{mm'}} \nabla z \cdot \tau_{nn'} \approx \begin{cases} \frac{|S_{mm'}|}{|S_{nn'}|}(z_{c_{m'}} - z_{c_m}), \text{ if } S_{nn'} \notin \partial\Omega_r, \\ \frac{|S_{mm'}|}{|S_{nn'}|}(\frac{z_{a_n} + z_{a_{n'}}}{2} - z_{c_m}), \text{ if } S_{nn'} \in \partial\Omega_r, \end{cases}$$

where $\partial\Omega_r$ is the boundary of the area covered the mobile sensor networks. This will lead to

$$\int\int_{C_m} f = \sum_{s\in(\partial C_m \cap \partial\Omega_r)} \frac{|S_{mm'}|}{\cos\theta_{s'}|S_{nn'}|}(\frac{z_{a_n} + z_{a_{n'}}}{2} - z_{c_m}) + \sum_{s\in(\partial C_m \setminus \partial\Omega_r)} \frac{|S_{mm'}|}{\cos\theta_{s'}|S_{nn'}|}(z_{c_{m'}} - z_{c_m}) - \sum_{s\in\partial C_m} \tan\theta_{s'}(z_{a_n} - z_{a_{n'}}). \tag{9}$$

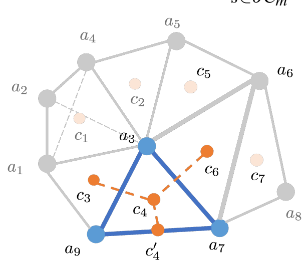

Fig. 5. Example of cell containing boundary edges of the network, which is cell C_4 in Fig. 1. Denote the middle point between a_9, a_7 as c'_4.

V. Distributed Estimation by Constrained Cooperative Kalman Filter

In this section, we will construct a distributed constrained cooperative Kalman filter using the local measurements to estimate the information at the cell center while incorporating the PDE information as a constraint to ensure the estimated information satisfying the PDE model.

A. Discrete Constraint Derived from the PDE Model

From the approximation results using FVM described in Section IV, we have the integral relationship described by (8) or (9) for any cell C_j. We observe that information of field values at both neighboring cell centers and adjacent agent locations at same time step are needed to have (8) or (9).

For cells of no boundary edges of the network, we rewrite (8) as

$$\sum_{s\in\partial C_j}\Big(-\tan\theta_s(z(r^k_{i,j},k) - z(r^k_{i',j},k)) + \frac{1}{\cos\theta_s}\frac{|S_{jj'}|}{|S_{ii'}|}(z(r^k_{c_{j'}},k) - z(r^k_{c_j},k))\Big) = \int\int_{C_j} f. \tag{10}$$

For cells containing boundary edges of the network, we rewrite (9) as

$$\int\int_{C_m} f = \sum_{s\in\partial C_m} -\tan\theta_{s'}(z(r^k_{n,m},k) - z(r^k_{n',m},k)) + \sum_{s\in(\partial C_m \setminus \partial\Omega_r)} \frac{1}{\cos\theta_{s'}}\frac{|S_{mm'}|}{|S_{nn'}|}(z(r^k_{C_{m'}},k) - z(r^k_{C_m},k)) + \sum_{s\in(\partial C_m \cap \partial\Omega_r)} \frac{1}{\cos\theta_{s'}}\frac{|S_{mm'}|}{|S_{nn'}|}(\frac{z(r^k_{n,m},k) + z(r^k_{n',m},k)}{2} - z(r^k_{C_m},k)). \tag{11}$$

Notice that if cell C_j has no boundary edges, then $\partial C_j \setminus \partial\Omega_r = \partial C_j$ and $\partial C_m \cap \partial\Omega_r = \emptyset$. Then (10) can also be written as (11) by replacing m, n with j, i respectively. Thus we rewrite (11) in linear form for any cell C_j

$$G^\intercal(j,k)x(j,k) = g(j,k), \tag{12}$$

where $x(j,k) = [z(r^k_{c_j},k), \nabla z(r^k_{c_j},k)]^\intercal$, $G(j,k) \triangleq \Big[\sum_{s\in\partial C_j} -\frac{|S_{jj'}|}{\cos\theta_s|S_{ii'}|} \quad 0_{1\times d}\Big]^\intercal$, and $g(j,k) \triangleq \int\int_{C_j} f + \sum_{s\in\partial C_j}\tan\theta_s(z(r^k_{i,j},k) - z(r^k_{i',j},k)) - \sum_{s\in(\partial C_j \setminus \partial\Omega_r)} \frac{|S_{jj'}|}{\cos\theta_s|S_{ii'}|} z(r^k_{c_{j'}},k) - \sum_{s\in(\partial C_j \cap \partial\Omega_r)} \frac{|S_{jj'}|}{\cos\theta_s|S_{ii'}|}\frac{z(r^k_{i,j},k) + z(r^k_{i',j},k)}{2}$.

B. Distributed Constrained Cooperative Kalman Filter

In order to estimate the information state of field value and gradient at each communication cell center, we will run a constrained cooperative Kalman filter locally for each cell, which makes our proposed solution distributed.

Assumption V.1 *We assume that the noises $e(j,k)$, $\varepsilon(j,k)$, $\boldsymbol{n}(j,k)$ are i.i.d. Gaussian noise with zero mean, and with constant covariance matrix for all j, i.e. $E[e(j,k)e^\intercal(j,k)] = W$, $E[\boldsymbol{n}(j,k)\boldsymbol{n}^\intercal(j,k)] = R_n$ and $E[\varepsilon(j,k)\varepsilon^\intercal(j,k)] = Q$.*

The constrained cooperative Kalman filter can be constructed using 6 steps:

(1) One-step state prediction

$$\hat{x}^-(j,k) = A(j,k-1)\tilde{x}^+(j,k-1) + U(j,k-1), \tag{13}$$

where $\tilde{x}^+(j,k-1)$ is the constrained state estimate from previous time step, and $\hat{x}^-(j,k)$ is the one-step state prediction.

(2) Error covariance of $\hat{x}^-(j,k)$

$$R^-(j,k) = A(j,k-1)R^+(j,k-1)A^\intercal(j,k-1) + W. \tag{14}$$

(3) Optimal gain

$$K(j,k) = R^-(j,k)C^\intercal(j,k)[C(j,k)R^-(j,k)C^\intercal(j,k) + D(j,k)QD^\intercal(j,k) + R_n]^{-1}. \tag{15}$$

(4) Updated unconstrained state estimate

$$\hat{x}^+(j,k) = \hat{x}^-(j,k) + K(j,k)(P(j,k) - C(j,k)\hat{x}^-(j,k) - D(j,k)\hat{H}(j,k)). \tag{16}$$

(5) Error covariance of $\hat{x}^+(j,k)$

$$(R^+(j,k))^{-1} = (R^-(j,k))^{-1} + C^\intercal(j,k)[D(j,k)QD^\intercal(j,k) + R_n]^{-1}C(j,k). \tag{17}$$

After running the 5 steps of the unconstrained filter, each cell obtains an unconstrained state estimate $\hat{x}^+(j,k)$ and it will share this information with all neighboring cells to update the constrained estimate.

Since there is no overlap between any pair of cells, the formation of the mobile sensor network satisfies $G^\intercal(j,k)G(j,k) = \left(\sum_{s\in\partial C_j} -\frac{|S_{jj'}|}{\cos\theta_s|S_{ii'}|}\right)^2 \neq 0, \forall j,k$.

(6) Updated constrained state estimate

$$\begin{aligned}\tilde{x}^+(j,k) &= \hat{x}^+(j,k) \\ &- G(j,k)(G^\intercal(j,k)G(j,k))^{-1}(G^\intercal(j,k)\hat{x}^+(j,k) - \hat{g}(j,k)),\end{aligned} \tag{18}$$

where $\hat{g}(j,k) \triangleq \iint_{C_j} f + \sum_{s\in\partial C_j}\tan\theta_s(p(r^k_{i,j},k) - p(r^k_{i',j},k)) - \sum_{s\in(\partial C_j\setminus\partial\Omega_r)}\frac{|S_{jj'}|\hat{z}^+(r^k_{c_{j'}},k)}{\cos\theta_s|S_{ii'}|} - \sum_{s\in(\partial C_j\cap\partial\Omega_r)}\frac{|S_{jj'}|}{\cos\theta_s|S_{ii'}|}\frac{p(r^k_{i,j},k)+p(r^k_{i',j},k)}{2}$ is an approximation of $g(j,k)$ with $\hat{z}^+(r^k_{c_{j'}},k) = \begin{bmatrix}1 & 0_{1\times d}\end{bmatrix}\hat{x}^+(j',k)$ and it uses measurements $p(r^k_{i,j},k), p(r^k_{i',j},k)$ as approximations for $z(r^k_{i,j},k), z(r^k_{i',j},k)$. According to the definition $G(j,k) = \begin{bmatrix}\sum_{s\in\partial C_j} -\frac{|S_{jj'}|}{\cos\theta_s|S_{ii'}|} & 0_{1\times d}\end{bmatrix}^\intercal$, the updated constrained estimate in (18) only updates the field value estimate $\hat{z}^+(r^k_{c_j},k)$, and does not affect the gradient estimate $\nabla\hat{z}^+(r^k_{c_j},k)$ obtained by (16).

Remark V.2 *For the 6 steps of the distributed constrained cooperative Kalman filter described by* (13)-(18)*, the first 5 steps in* (13)-(17) *only use the local information in one communication cell, while the last step* (18) *uses estimated information from neighboring cells.*

VI. Convergence Analysis

In this section, we will provide convergence analysis for the proposed distributed constrained cooperative filter.

Agents from same cell have all-to-all communication. The information dynamics and measurement equation considered for each individual cell in this paper share the same structure as those in [10], where a centralized cooperative Kalman filter has been proposed with provable convergence. If we do not consider the constraints, then the unconstrained distributed cooperative Kalman filter for each single cell is convergent if conditions in Proposition VI.1 and Proposition VI.2 are all satisfied.

Proposition VI.1 *(Lemma 3.5 in [10]) The state dynamics* (3) *are uniformly completely controllable if the following conditions are satisfied:*
(Cd1) The covariance matrix W is bounded, i.e., $\lambda_1 I \leq W \leq \lambda_2 I$ for some constants $\lambda_1,\lambda_2 > 0$.
(Cd2) The speed of each agent is uniformly bounded, i.e., $\|r^k_{i,j} - r^{k-1}_{i,j}\|_2 \leq \lambda_3$ for all i,j,k, and some constant $\lambda_3 > 0$.

Proposition VI.2 *(Lemma 3.8 in [10]) The state dynamics* (3) *with the measurement equation* (6) *are uniformly completely observable if (Cd2) and the following conditions are satisfied:*
(Cd3) The number of agents in one cell C_j satisfies $|C_j| > d$ for all j.
(Cd4) The covariance matrices R_n and Q are bounded, i.e., $\lambda_4 I \leq R_n \leq \lambda_5 I$ and $0 \leq Q \leq \lambda_6 I$ for some $\lambda_4,\lambda_5,\lambda_6 > 0$.
(Cd5) The distance between each agent and the formation center is uniformly bounded from both above and below, i.e., $\lambda_7 \leq \|r^k_{i,j} - r^k_{c_j}\|_2 \leq \lambda_8$ for all i,j,k, and some $\lambda_7,\lambda_8 > 0$.
(Cd6) There exists a constant time difference δt, and for all $k > \delta t$, there exists a time instance $k' \in [k-\delta t, k]$, as well as two agents i_1, i_2 from cell C_j, such that $(r^{k'}_{i_1,j} - r^{k'}_{c_j})$ and $(r^{k'}_{i_2,j} - r^{k'}_{c_j})$ are linearly independent.

Since the unconstrained cooperative Kalman filter is both uniformly complete controllable (Proposition VI.1) and observable (Proposition VI.2), the unconstrained filter for each individual cell is convergent. This means that $\|x_j - \hat{x}_j\|_2$ is bounded for all j, where x_j represents the true state value.

Define a combined state vector $X(k)$ to include all distributed state vectors as $X(k) = \left[x^\intercal(1,k),\cdots,x^\intercal(N,k)\right]^\intercal$, which represents the true state value. Similarly we can have updated unconstrained combined state estimate $\hat{X}^+(k) = \left[\hat{x}^+(1,k)^\intercal,\cdots,\hat{x}^+(N,k)^\intercal\right]^\intercal$ and constrained combined state estimate $\tilde{X}^+(k) = \left[\tilde{x}^+(1,k)^\intercal,\cdots,\tilde{x}^+(N,k)^\intercal\right]^\intercal$. Then we can have one constrained cooperative Kalman filter of $X(k)$ as

$$\begin{aligned}
&\hat{X}^-(k) = A(k-1)\tilde{X}^+(k-1) + U(k-1),\\
&R^-(k) = A(k-1)R^+(k-1)A^\intercal(k-1) + W,\\
&K(k) = R^-(k)C^\intercal(k)[C(k)R^-(k)C^\intercal(k) + D(k)QD^\intercal(k) + R]^{-1},\\
&\hat{X}^+(k) = \hat{X}^-(k) + K(k)(P(k) - C(k)\hat{x}^-(k) - D(k)\hat{H}(k)),\\
&(R^+(k))^{-1} = (R^-(k))^{-1} + C^\intercal(k)[D(k)QD^\intercal(k) + R]^{-1}C(k),\\
&\tilde{X}^+(k) = \hat{X}^+(k) - G(k)(G^\intercal(k)G(k))^{-1}(G^\intercal(k)\hat{x}^+(k) - \hat{g}(k)),
\end{aligned}$$

where $A(k) = \mathrm{diag}(A(1,k),\cdots,A(N,k))$, $C(k) = \mathrm{diag}(C(1,k),\cdots,C(N,k))$, $D(k) = \left[D^\intercal(1,k),\cdots,D^\intercal(N,k)\right]^\intercal$, $P(k) = \left[P^\intercal(1,k),\cdots,P^\intercal(N,k)\right]^\intercal$, $G(k) = \mathrm{diag}(G(1,k),\cdots,G(N,k))$, $\hat{g}(k) = \left[\hat{g}(1,k),\cdots,\hat{g}(N,k)\right]^\intercal$. Since the combined filter is constructed by stacking all distributed filter together and the unconstrained filter for each individual cell is convergent, the combined unconstrained filter is also convergent as $\|X - \hat{X}\|_2 = \sqrt{\sum_{j=1}^N \|x - x_j\|_2^2} \leq \sum_{j=1}^N \|x - x_j\|_2$. By Theorem 4 in [17], $\|X - \tilde{X}^+\|_2 \leq \|X - \hat{X}^+\|_2$, where $\|\cdot\|_2$ is the l_2 norm. Since the unconstrained combined cooperative Kalman filter is convergent, the constrained combined cooperative Kalman filter is also convergent. Thus, each distributed constrained cooperative Kalman filter is convergent.

VII. Simulation Results

In this section, a simulation using a mobile sensor network (with formation shown in Fig. 6) will be provided to demonstrate that the proposed distributed algorithm enables mobile sensor networks to estimate information at each cell center along trajectories of a collection of cell centers.

We consider a electric potential field in $\mathbb{R}^2$ described by the Poisson equation $\nabla^2 z(r,t) = \frac{\rho}{\varepsilon_0}$ where ρ is a total volume charge density and ε_0 is the permittivity of the medium. We place the point charge at $[0,0]^\intercal$. The center of the mobile sensor networks is moving in a fixed formation shown in Fig.

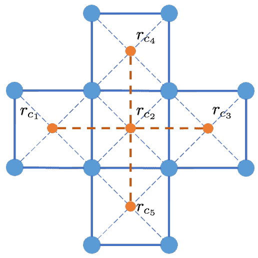

Fig. 6. A mobile sensor network with 5 square communication cells. Blue nodes represent sensor, and orange nodes represent cell centers. Blue solid lines represent cell boundary edges and blue dashed ones represent communication edges inside one cell. Orange dashed lines represent information sharing between neighboring cell centers.

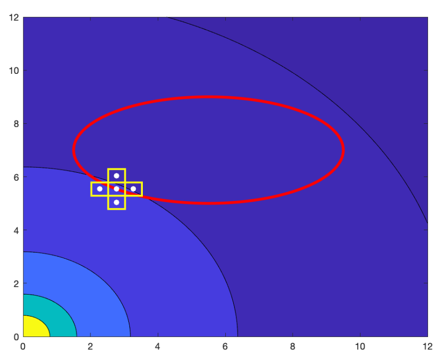

Fig. 7. A 5-cell mobile sensor network follows an elliptical trajectory in an electric potential field. The red ellipse represents the trajectory, the yellow lines represent boundary edges, and white dots represent cell centers.

6 with the velocity $v(t) = [-\frac{1}{5\pi}\sin(\frac{t}{20\pi}), \frac{1}{10\pi}\cos(\frac{t}{20\pi})]^\intercal$ for 2000s. The trajectory of r_{c_2} satisfies $(r_x - 5.5)^2 + 4(r_y - 7)^2 = 16$ where $r_{c_2} = [r_x, r_y]^\intercal$ as shown in Fig. 7. Each boundary edge for one single cell has length 0.5.

Statistical data of estimation errors at cell centers are provided in Table I along with the data of measurement noise. The subscript n represents measurement noise, and the subscript e represents constrained estimation error. From

TABLE I

STATISTICAL DATA OF ESTIMATION ERRORS AND NOISE

	Cell C_1	Cell C_2	Cell C_3	Cell C_4	Cell C_5
$mean_n$	-0.0012	-0.0013	-0.0014	0.0009	0.0017
$mean_e$	-0.0021	0.0003	0.0028	0.0041	-0.0041
std_n	0.0579	0.0589	0.0588	0.0586	0.0581
std_e	0.0243	0.0245	0.0242	0.0245	0.0245

Table I, we can observe that the mean for the constrained estimation error is close to zero for each cell, which means that the estimation generated by the constrained distributed cooperative Kalman filter is accurate. The estimation for cell C_2 is more accurate compared with the estimation for the other cells. This is because cell C_2 is the center cell of the mobile sensor network, and it exchanges information with all other cells while other cells only share information with cell C_2, as shown in Fig. 6. Besides, the standard deviation of the constrained estimation error is smaller than that of measurement noise, which demonstrates that distributed constrained cooperative Kalman filter is capable of reducing the noise and providing accurate estimation.

VIII. Conclusion and Future Work

In this paper, we propose a distributed cooperative Kalman filter under constraints induced by the Poisson equation. The method enables a large number of mobile sensors to be leveraged for mapping a spatial-temporal field. Our results demonstrate that the finite volume method is an effective tool to convert PDEs into a spatial-temporal relationship that can be leveraged by mobile sensor networks. We will generalize our method to other types of PDEs in future work.

References

[1] M. Eshghi and H. R. Schmidtke, "An approach for safer navigation under severe hurricane damage," *Journal of Reliable Intelligent Environments*, vol. 4, no. 3, pp. 161–185, 2018.

[2] C. Wei, H. G. Tanner, X. Yu, and M. A. Hsieh, "Low-range interaction periodic rendezvous along lagrangian coherent structures," in *2019 American Control Conference (ACC)*. IEEE, 2019, pp. 4012–4017.

[3] J. Chen and P. Dames, "Distributed and collision-free coverage control of a team of mobile sensors using the convex uncertain voronoi diagram," in *2020 American Control Conference (ACC)*. IEEE, 2020, pp. 5307–5313.

[4] H. Park, J. Liu, M. Johnson-Roberson, and R. Vasudevan, "Robust environmental mapping by mobile sensor networks," in *2018 IEEE International Conference on Robotics and Automation (ICRA)*. IEEE, 2018, pp. 2395–2402.

[5] A. Sommerfeld, *Partial differential equations in physics*. Academic press, 1949.

[6] S. Koga and M. Krstic, "Arctic sea ice state estimation from thermodynamic pde model," *Automatica*, vol. 112, p. 108713, 2020.

[7] M. A. Demetriou, "Employing mobile sensor density to approximate state feedback kernels in static output feedback control of pdes," in *2021 American Control Conference (ACC)*. IEEE, 2021, pp. 2775–2781.

[8] P. K. Mishra, D. Chatterjee, and D. E. Quevedo, "Stochastic predictive control under intermittent observations and unreliable actions," *Automatica*, vol. 118, p. 109012, 2020.

[9] W. Hu, M. A. Demetriou, X. Tian, and N. A. Gatsonis, "Hybrid domain decomposition filters for advection–diffusion pdes with mobile sensors," *Automatica*, vol. 138, p. 110109, 2022.

[10] F. Zhang and N. E. Leonard, "Cooperative filters and control for cooperative exploration," *IEEE Transactions on Automatic Control*, vol. 55, no. 3, pp. 650–663, 2010.

[11] J. You, Z. Zhang, F. Zhang, and W. Wu, "Cooperative filtering and parameter identification for advection–diffusion processes using a mobile sensor network," *IEEE Transactions on Control Systems Technology*, 2022.

[12] W. Wu, J. You, Y. Zhang, M. Li, and K. Su, "Parameter identification of spatial–temporal varying processes by a multi-robot system in realistic diffusion fields," *Robotica*, vol. 39, no. 5, p. 842–861, 2021.

[13] Z. Zhang, W. Wu, and F. Zhang, "Cooperative filtering and parameter estimation for polynomial pdes using a mobile sensor network," in *2022 American Control Conference (ACC)*. IEEE, 2022, pp. 982–987.

[14] F. Hermeline, "A finite volume method for the approximation of diffusion operators on distorted meshes," *Journal of computational Physics*, vol. 160, no. 2, pp. 481–499, 2000.

[15] J. Droniou, "Finite volume schemes for diffusion equations: Introduction to and review of modern methods," *Mathematical Models and Methods in Applied Sciences*, vol. 24, no. 8, pp. 1575–1619, 2014.

[16] F. Hermeline, "A finite volume method for the approximation of convection–diffusion equations on general meshes," *International Journal of Numerical Methods in Engineering*, vol. 91, pp. 1331–1357, 2012.

[17] D. Simon and T. L. Chia, "Kalman filtering with state equality constraints," *IEEE transactions on Aerospace and Electronic Systems*, vol. 38, no. 1, pp. 128–136, 2002.